Tenth-order QED contribution to lepton anomalous magnetic moment: Fourth-order vertices containing sixth-order vacuum-polarization subdiagrams

Tatsumi Aoyama,[1,2] Masashi Hayakawa,[2,3] Toichiro Kinoshita,[2,4] and Makiko Nio[2]

[1]*Kobayashi-Maskawa Institute for the Origin of Particles and the Universe (KMI), Nagoya University, Nagoya, 464-8602, Japan*
[2]*Theoretical Physics Laboratory, Nishina Center, RIKEN, Wako, 351-0198, Japan*
[3]*Department of Physics, Nagoya University, Nagoya, 464-8602, Japan*
[4]*Laboratory for Elementary-Particle Physics, Cornell University, Ithaca, New York, 14853, USA*
(Received 12 January 2011; published 7 March 2011)

This paper reports the tenth-order contributions to the $g - 2$ of the electron a_e and those of the muon a_μ from the gauge-invariant Set II(c), which consists of 36 Feynman diagrams, and Set II(d), which consists of 180 Feynman diagrams. Both sets are obtained by insertion of sixth-order vacuum-polarization diagrams in the fourth-order anomalous magnetic moment. The mass-independent contributions from Set II(c) and Set II(d) are $-0.116\,489\,(32)(\alpha/\pi)^5$ and $-0.243\,00\,(29)(\alpha/\pi)^5$, respectively. The leading contributions to a_μ, which involve electron loops only, are $-3.888\,27\,(90)(\alpha/\pi)^5$ and $0.4972\,(65)(\alpha/\pi)^5$ for Set II(c) and Set II(d), respectively. The total contributions of the electron, muon, and tau-lepton loops to a_e are $-0.116\,874\,(32)(\alpha/\pi)^5$ for the Set II(c), and $-0.243\,10\,(29)(\alpha/\pi)^5$ for the Set II(d), respectively. The contributions of the electron, muon, and tau-lepton loop to a_μ are $-5.5594\,(11)(\alpha/\pi)^5$ for the Set II(c) and $0.2465\,(65)(\alpha/\pi)^5$ for the Set II(d), respectively.

I. INTRODUCTION

The anomalous magnetic moment $g - 2$ of the electron has played the central role in testing the validity of quantum electrodynamics (QED) as well as the standard model. The latest measurement of $a_e \equiv (g - 2)/2$ by the Harvard group has reached the precision of 0.24×10^{-9} [1,2]:

$$a_e(\text{HV08}) = 1\,159\,652\,180.73\,(0.28) \times 10^{-12} \quad [0.24\,\text{ppb}]. \tag{1}$$

At present the best prediction of theory consists of QED corrections of up to the eighth order [3–5], and hadronic corrections [6–12] and electroweak corrections [13–15] scaled down from their contributions to the muon $g - 2$. To compare the theoretical prediction with the experiment (1), we also need the value of the fine structure constant α determined by a method independent of $g - 2$. The best value of such an α has been obtained recently from the measurement of h/m_{Rb}, the ratio of the Planck constant and the mass of the Rb atom, combined with the very precisely known Rydberg constant and m_{Rb}/m_e [16]:

$$\alpha^{-1}(\text{Rb10}) = 137.035\,999\,037\,(91) \quad [0.66\,\text{ppb}]. \tag{2}$$

With this α the theoretical prediction of a_e becomes

$$a_e(\text{theory}) = 1\,159\,652\,181.13\,(0.11)(0.37)(0.77) \times 10^{-12}, \tag{3}$$

where the first, second, and third uncertainties come from the calculated eighth-order QED term, the tenth-order estimate, and the fine structure constant (2), respectively.

The theory (3) is thus in good agreement with the experiment (1),

$$a_e(\text{HV08}) - a_e(\text{theory}) = -0.40\,(0.88) \times 10^{-12}, \tag{4}$$

proving that QED (standard model) is in good shape even at this very high precision.

An alternative test of QED is to compare the α of (2) with the value of α determined from the experiment and theory of $g - 2$:

$$\alpha^{-1}(a_e08) = 137.035\,999\,085\,(12)(37)(33) \quad [0.37\,\text{ppb}], \tag{5}$$

where the first, second, and third uncertainties come from the eighth-order QED term, the tenth-order estimate, and the measurement of $a_e(\text{HV08})$, respectively. Although the uncertainty of $\alpha^{-1}(a_e08)$ in (5) is a factor 2 smaller than $\alpha^{-1}(\text{Rb10})$, it is not a firm factor since it depends on the estimate of the tenth-order term, which is only a crude guess [17]. In anticipation of this challenge we launched a systematic program several years ago to evaluate the complete tenth-order term [18–20].

The tenth-order QED contribution to the anomalous magnetic moment of an electron can be written as

$$a_e^{(10)} = \left(\frac{\alpha}{\pi}\right)^5 [A_1^{(10)} + A_2^{(10)}(m_e/m_\mu) + A_2^{(10)}(m_e/m_\tau) + A_3^{(10)}(m_e/m_\mu, m_e/m_\tau)], \tag{6}$$

where the electron-muon mass ratio m_e/m_μ is $4.836\,331\,71\,(12) \times 10^{-3}$ and the electron-tau mass ratio m_e/m_τ is $2.875\,64\,(47) \times 10^{-4}$ [17]. The contribution to
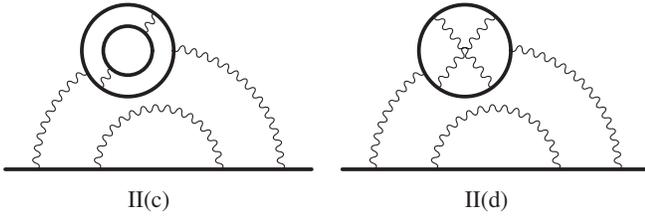
FIG. 1.   Typical diagrams of the tenth-order Set II(c) and Set II(d).

FIG. 3.   Self-energy-like diagrams of fourth order.

the mass-independent term $A_1^{(10)}$ coming from 12 672 Feynman diagrams may be classified into six gauge-invariant sets, further divided into 32 gauge-invariant subsets depending on the nature of closed lepton loop subdiagrams. Thus far, results of numerical evaluation of 24 gauge-invariant subsets, which consist of 2785 vertex diagrams, have been published [5,21–24]. The result of 105 vertex diagrams of Set I(i) has been recently submitted for publication [25]. Five of the subsets had also been calculated analytically [26,27]. Our calculation is in good agreement with these analytic results.

In this article we report the evaluation of contributions of two gauge-invariant subsets, Set II(c) and Set II(d), which consist of fourth-order vertex diagrams containing vacuum-polarization subdiagrams of sixth order. The effect of insertion of a gauge-invariant set of closed lepton loops in an internal photon line of momentum q is expressed by the renormalized vacuum-polarization tensor of the form

$$\Pi^{\mu\nu}(q) = (q^\mu q^\nu - q^2 g^{\mu\nu})\Pi(q^2), \qquad (7)$$

where the scalar vacuum-polarization function $\Pi(q^2)$ vanishes at $q^2 = 0$ on carrying out the charge renormalization.

The Set II(c) consists of 36 Feynman diagrams. A typical diagram of this set is shown on the left-hand side of Fig. 1. It is obtained by insertion of proper sixth-order vacuum-polarization diagrams containing two closed lepton loops (see Fig. 2) in the fourth-order anomalous magnetic moment M_{4a} or M_{4b} represented by Fig. 3. These diagrams can be represented by 4 independent integrals taking account of various symmetry properties.
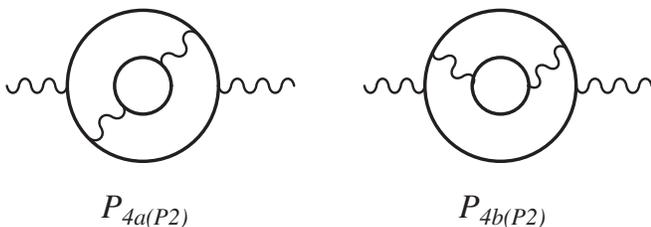

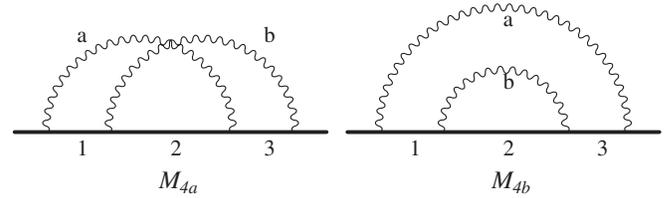FIG. 2.   Sixth-order vacuum-polarization diagrams consisting of two fermion loops.

The Set II(d) consists of 180 Feynman diagrams. A typical diagram of this set is shown on the right-hand side of Fig. 1. It is obtained by insertion of proper sixth-order vacuum-polarization diagrams consisting of one closed lepton loop in the fourth-order anomalous magnetic moment. These diagrams can be represented by 16 independent integrals taking account of various symmetry properties.

Evaluation of the contribution of the Set II(c) to the mass-independent term $A_1^{(10)}$ is straightforward since an exact spectral function $\Pi^{(4,2)}$ for the diagrams of Fig. 2 is known for the diagrams whose two lepton loops have the same mass [28]. However, evaluation of the mass-dependent term $A_2^{(10)}$ requires $\Pi^{(4,2)}$ as a function of m_e/m_μ or m_e/m_τ, which is not available at present. In order to cover both cases, we follow an alternative approach [29] in which we construct a Feynman-parametric integral of the sixth-order vacuum-polarization function $\Pi^{(4,2)}$ and insert it in the virtual photon lines of the Feynman-parametric integral of the fourth-order anomalous magnetic moment M_4.

For the Set II(d) an exact vacuum-polarization function $\Pi^{(6)}$ (see Fig. 4) is not known, although the Padé approximant is known to provide a good approximation [30–32]. We follow here primarily the approach [29] which utilizes the vacuum-polarization function $\Pi^{(6)}$ itself, instead of its spectral function. The calculation utilizing the Padé approximant of the spectral function is also carried out to provide an independent check.

Parametric representations of several vacuum-polarization functions are presented in Sec. II, where explicit definitions of functions are given. As an illustration of our approach, insertion of the vacuum-polarization function in M_2 is presented in Sec. III. Insertion of $\Pi^{(2)}$, $\Pi^{(4)}$, $\Pi^{(4,2)}$, and $\Pi^{(6)}$ in M_4 is described in Sec. IV. Although most results of Secs. II and III are concerned with quantities of low orders, they are needed in carrying out the renormalization of the tenth-order terms. In cases where the spectral function is available, we present alternative ways which provide a consistency check of the numerical work. Application of these methods to Set II(c) and Set II(d) is described in Secs. V and VI. Summary and concluding remarks are presented in Sec. VII. For simplicity the factor $(\alpha/\pi)^5$ is omitted in Secs. II, III, IV, V, and VI.
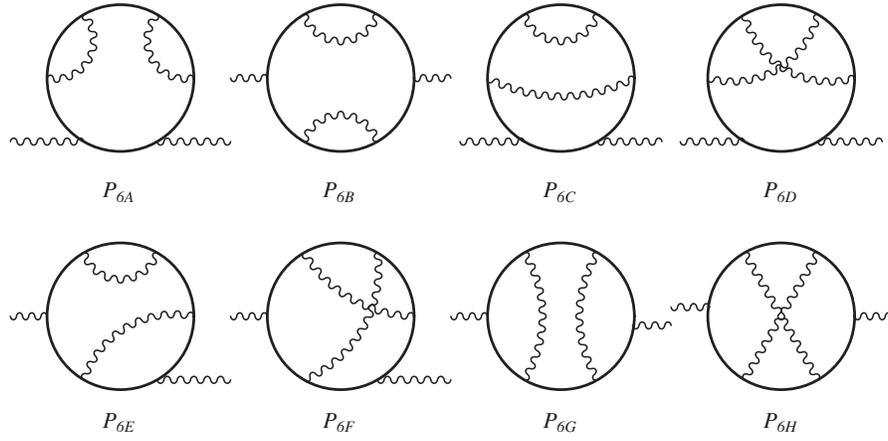
FIG. 4. Sixth-order vacuum-polarization diagrams consisting of a single fermion loop.

II. PARAMETRIC REPRESENTATION OF VACUUM-POLARIZATION FUNCTION

As is shown in Ref. [29] the second-order vacuum-polarization function can be written in the form

$$\Pi^{(2)}(x) = \int (dz) \frac{D_0}{U^2} \ln\left(\frac{V_0}{V}\right), \qquad (8)$$

with

$$(dz) = dz_1 dz_2 \delta(1 - z_{12}), \qquad U = z_{12}, \qquad V_0 = z_{12}m_1^2,$$

$$V = V_0 - xG, \qquad\qquad x = q^2, \qquad G = z_1 A_1,$$

$$A_1 = z_2/U, \qquad\qquad D_0 = 2A_1(1 - A_1), \qquad (9)$$

where z_1 and z_2 are Feynman parameters of leptons forming the loop, $z_{12} = z_1 + z_2$, and m_1 is the rest mass of the lepton.

As a preparation for constructing $\Pi^{(4,2)}$ let us first construct the parametric integral of the fourth-order vacuum-polarization function $\Pi^{(4)}$. It has contributions from one diagram P_{4a} and two diagrams P_{4b} of Fig. 5.

The contribution of P_{4a}, renormalized at $q = 0$ but with subvertex divergences not yet removed, can be written as [29]

$$\Pi^{(4a)}(x) = \int (dz) \left[\frac{D_0}{U^2}\left(\frac{1}{V} - \frac{1}{V_0}\right) + \frac{D_1}{U^3}\ln\left(\frac{V_0}{V}\right) \right], \quad (10)$$
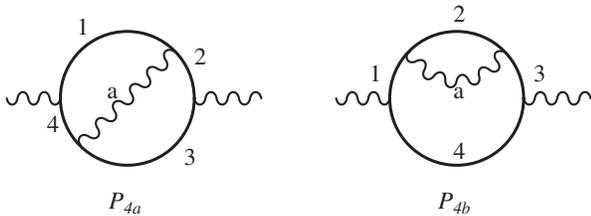

FIG. 5. Fourth-order vacuum-polarization diagrams consisting of one lepton loop.

where z_1, z_2, z_3, z_4 are Feynman parameters for the electron lines and z_a is that of the photon line and

$$(dz) = dz_1 dz_2 dz_3 dz_4 dz_a \delta(1 - z_{1234a}), \qquad z_i \geq 0,$$

$$B_{11} = z_{23a}, \qquad B_{12} = z_a, \qquad B_{22} = z_{14a},$$

$$U = z_{14}B_{11} + z_{23}B_{12}, \qquad A_1 = (z_3 B_{12} + z_4 B_{11})/U,$$

$$A_2 = (z_3 B_{22} + z_4 B_{12})/U, \qquad A_3 = A_2 - 1,$$

$$A_4 = A_1 - 1, \qquad V_0 = z_{1234}m_1^2 + \lambda^2 z_a,$$

$$G = z_1 A_1 + z_2 A_2, \qquad V = V_0 - xG, \qquad x = q^2,$$

$$D_0 = ((A_1 + A_4)(A_2 + A_3) - A_1 A_4 - A_2 A_3)m_1^2,$$

$$D_1 = (A_1 A_2 + A_3 A_4)B_{12} - A_1 A_4 B_{22} - A_2 A_3 B_{11}. \quad (11)$$

Here $z_{23a} = z_2 + z_3 + z_a$, etc., and λ is the (infinitesimal) photon mass.

This integral contains ultraviolet (UV) divergences arising from the vertex diagrams $\{2, 3, a\}$ and $\{1, 4, a\}$, which can be removed by the K_{23} operation and K_{14} operation [29], respectively. The renormalized function $\Pi_{\text{ren}}^{(4a)}$ can be written as

$$\Pi_{\text{ren}}^{(4a)} = \Delta\Pi^{(4a)} - 2L_2^{\text{R}}\Pi^{(2)}, \qquad (12)$$

where

$$\Delta\Pi^{(4a)} = (1 - K_{23} - K_{14})\Pi^{(4a)}. \qquad (13)$$

$\Pi^{(2)}$ is the second-order vacuum-polarization function given by Eq. (8), and $L_2^{\text{R}} \equiv L_2 - L_2^{\text{UV}}$, where L_2^{UV} is the UV-divergent part of the second-order vertex-renormalization constant L_2 defined by the K operation and L_2^{R} is the remainder including an infrared divergent part of L_2.

The renormalized vacuum-polarization term coming from P_{4b} of Fig. 5 may be handled similarly by the K operation [29]. It leads to

$$\Pi_{\text{ren}}^{(4b)} = \Delta\Pi^{(4b)} - 2B_2^{\text{R}}\Pi^{(2)}, \qquad (14)$$

where $B_2^R = B_2 - B_2^{UV}$ [29] and

$$\Delta\Pi^{(4b)}(x) = \int (dz)(1 - K_2)\left[\frac{D_0}{U^2}\left(\frac{1}{V} - \frac{1}{V_0}\right) + \frac{xC_0}{U^2 V}\right.$$
$$\left. + \frac{D_1}{U^3}\ln\left(\frac{V_0}{V}\right)\right], \quad (15)$$

with

$$B_{11} = z_{2a}, \qquad B_{12} = z_a, \qquad B_{22} = z_{134a},$$
$$U = z_{134}B_{11} + z_2 B_{12}, \qquad A_1 = z_4 B_{11}/U,$$
$$A_2 = z_4 B_{12}/U, \qquad A_3 = A_1, \qquad A_4 = A_1 - 1,$$
$$G = z_{13}A_1 + z_2 A_2, \qquad V = V_0 - xG, \qquad x = q^2,$$
$$D_0 = (4A_1 - A_2)A_4 m_1^2, \qquad C_0 = -A_1^2 A_2 A_4,$$
$$D_1 = A_1(A_1 + 3A_4)B_{12}. \quad (16)$$

V_0 and (dz) have the same form as in (11).

The function $\Pi^{(4,2)}$ is obtained readily from $\Pi^{(4)}$ by insertion of the spectral representation of the vacuum-polarization loop

$$\frac{\Pi(q^2)}{q^2} = \int_0^1 dt\,\frac{\rho(t)}{-q^2 + 4m_2^2/(1 - t^2)}, \quad (17)$$

in the virtual photon line of $\Pi^{(4)}$ carrying momentum q. This equation can be regarded as a superposition of vector particles of mass $4m_2^2/(1 - t^2)$, where m_2 is the mass of the inserted loop particle. The net effect is expressed as the replacement

$$\frac{1}{q^2} \to \int_0^1 dt\,\frac{\rho(t)}{q^2 - 4m_2^2/(1 - t^2)}. \quad (18)$$

For the second-order electron loop the spectral function is given by [29]

$$\rho^{(2)}(t) = \frac{t^2(1 - t^2/3)}{1 - t^2}. \quad (19)$$

From (10) and (18) we obtain

$$\Delta\Pi^{(4a,2)}(x) = \int_0^1 dt\,\rho^{(2)}(t)\int (dz)(1 - K_{23} - K_{14})$$
$$\times\left[\frac{D_0}{U^2}\left(\frac{1}{V} - \frac{1}{V_0}\right) + \frac{D_1}{U^3}\ln\left(\frac{V_0}{V}\right)\right], \quad (20)$$

where $x = q^2$, and D_0 and D_1 are given in Eq. (11). V_0 and V have the form

$$V = V_0 - xG, \qquad x = q^2,$$
$$V_0 = z_{1234}m_1^2 + z_a\frac{4m_2^2}{1 - t^2}. \quad (21)$$

Similarly, from (15) and (18), we obtain

$$\Delta\Pi^{(4b,2)}(x) = \int_0^1 dt\,\rho^{(2)}(t)\int (dz)(1 - K_2)\left[\frac{D_0}{U^2}\left(\frac{1}{V} - \frac{1}{V_0}\right)\right.$$
$$\left. + \frac{xC_0}{U^2 V} + \frac{D_1}{U^3}\ln\left(\frac{V_0}{V}\right)\right], \quad (22)$$

where D_0, C_0, and D_1 are given in Eq. (16), and V and V_0 are given by (21).

In the same manner as in (10) and (15) the sixth-order vacuum-polarization function $\Pi^{(6)}(q^2)$ can be written in the general form [29]

$$\Delta\Pi^{(6)}(x) = \int (dz)\left[\frac{D_0}{U^2}\left(\frac{1}{V^2} - \frac{1}{V_0^2}\right) + \frac{x(B_0 + xC_0)}{U^2 V^2}\right.$$
$$\left. + \frac{D_1}{U^3}\left(\frac{1}{V} - \frac{1}{V_0}\right) + \frac{xB_1}{U^3 V} + \frac{D_2}{U^4}\ln\left(\frac{V_0}{V}\right)\right], \quad (23)$$

where

$$V_0 = z_{123456}m_1^2, \quad (24)$$

and D_0 is m_1^4 times D_0, and B_0 and D_1 are m_1^2 times B_0 and D_1, given in Ref. [33]. For simplicity the K operation is not shown explicitly. For the sixth-order vacuum-polarization diagrams P_{6C} and P_{6D} of Fig. 4, which contain fourth-order lepton self-energy subdiagrams, the K operation subtracts only UV-divergent parts δm_{4a}^{UV} and δm_{4b}^{UV}, which are different from the full mass-renormalization terms δm_{4a} and δm_{4b}. This causes no problem for the renormalization of the vacuum-polarization function which has no infrared divergence. However, the fully renormalized formula is simpler if the residual mass-renormalization terms $\delta m_{4a}^R (\equiv \delta m_{4a} - \delta m_{4a}^{UV})$ and $\delta m_{4b}^R (\equiv \delta m_{4b} - \delta m_{4b}^{UV})$ are also subtracted. This subtraction is performed by the R subtraction method introduced in Ref. [19]. We shall therefore include the R subtraction operation in Eq. (23) whenever it is needed.

III. INSERTION OF VACUUM-POLARIZATION FUNCTION INTO THE SECOND-ORDER ANOMALY

Before discussing insertion of the vacuum-polarization (VP) diagram in M_4, let us consider insertion in M_2. The Feynman-parametric representation of the second-order magnetic moment can be written in the form [29]

$$M_2 = \int \frac{(dy)}{U_y^2}\frac{F_0}{V_y}, \quad (25)$$

where y_1 and y_a are Feynman parameters of the electron line and the photon line, respectively,

$$(dy) = dy_1 dy_a \delta(1 - y_{1a}), \qquad y_{1a} = y_1 + y_a,$$
$$U_y = y_{1a}B_{11}, \qquad B_{11} = 1,$$
$$A_1 = y_a/U_y, \qquad V_y = y_1 - y_1 A_1, \quad (26)$$
$$F_0 = y_1 A_1(1 - A_1),$$

and the rest mass of the open electron line (or, open lepton line) is chosen to be 1. The insertion of the vacuum-polarization function Π into the photon line a can be written as

$$M_{2,P} = \int_0^1 dt \rho(t) \int \frac{(dy)}{U_y^2} \frac{F_0}{V_y + 4m_1^2 y_a (1-t^2)^{-1}}, \quad (27)$$

following Eq. (18). Comparing (27) with (17), we can write

$$\begin{aligned} M_{2,P} &= \int \frac{(dy)}{U_y^2} \frac{F_0}{y_a} \int_0^1 dt \frac{\rho(t)}{V_y/y_a + 4m_1^2(1-t^2)^{-1}} \\ &= \int \frac{(dy)}{U_y^2} \frac{F_0}{y_a} \frac{\Pi(q^2)}{q^2} \bigg|_{q^2 = -V_y/y_a} \\ &= -\int \frac{(dy)}{U_y^2} \frac{F_0}{V_y} \Pi(-V_y/y_a). \end{aligned} \quad (28)$$

This gives us a simple and transparent recipe for insertion of the vacuum-polarization function in the photon line a of M_2:

$$\frac{1}{V_y} \rightarrow -\frac{1}{V_y} \Pi(-V_y/y_a). \quad (29)$$

This is identical to Eq. (5.8) on p. 285 of Ref. [29] noting that

$$V_0 = z_{12} m_1^2, \quad V = V_0 - xG|_{x=-V_y/y_a}, \quad W = \frac{V}{V - V_0}. \quad (30)$$

Note that this derivation requires only the analytic property expressed by the spectral representation. No actual knowledge of the spectral function is required.

Making use of Eq. (29) and the form of $\Pi^{(2)}(x)$ given by Eq. (8), M_{2,P_2} can be readily written in the form

$$\begin{aligned} M_{2,P_2} &= -\int_0^1 dy(1-y) \int (dz) \frac{D_0}{U^2} \ln\left(\frac{V_0}{V}\right), \\ x &= -\frac{V_y}{y_a} = -\frac{y^2}{1-y}, \end{aligned} \quad (31)$$

where $y = y_1$, $y_a = 1 - y_1$, and $V = V_0 - xG$.

In the case $P = P_4$, we obtain from Eq. (15)

$$\begin{aligned} M_{2,P_4} &= -\int_0^1 dy(1-y) \int (dz) \Big[\frac{D_0}{U^2}\left(\frac{1}{V} - \frac{1}{V_0}\right) \\ &\quad + \frac{xC_0}{U^2 V} + \frac{D_1}{U^3} \ln\left(\frac{V_0}{V}\right) \Big]_{x=-y^2/(1-y)}, \end{aligned} \quad (32)$$

where $V_0 = z_{1234} m_1^2$ and $V = V_0 - xG$. K operation (and R subtraction) is not shown explicitly for simplicity. This corresponds to Eq. (5.20) on p. 288 of Ref. [29] noting that

$$V_0 = z_{12} m_1^2, \quad V = V_0 - xG|_{x=-V_y/y_a}, \quad W = \frac{V}{V - V_0}. \quad (33)$$

Similarly, for insertion of $P = P_6$, we have the general structure

$$\begin{aligned} M_{2,P_6} &= \int_0^1 dy(1-y) \int (dz) \Big[\frac{D_0}{U^2}\left(\frac{1}{V^2} - \frac{1}{V_0^2}\right) \\ &\quad + \frac{xB_0 + x^2 C_0}{U^2 V^2} + \frac{D_1}{U^3}\left(\frac{1}{V} - \frac{1}{V_0}\right) + \frac{xB_1}{U^3 V} \\ &\quad + \frac{D_2}{U^4} \ln\left(\frac{V_0}{V}\right) \Big]_{x=-y^2/(1-y)}, \end{aligned} \quad (34)$$

where V_0 is given in Eq. (24). This equation, with $m_1^2 = 1$, corresponds to Eq. (5.32) on p. 293 of Ref. [29] except that it includes R subtractions besides K operations for some diagrams.

IV. INSERTION OF VACUUM-POLARIZATION FUNCTION INTO A FOURTH-ORDER MAGNETIC MOMENT

The fourth-order magnetic moment M_4, which consists of two parts M_{4a} and M_{4b}, has the form [29]

$$M_4 = \int (dy) \Big[\frac{E_0 + \tilde{C}_0}{U_y^2 V_y} + \frac{N_0 + Z_0}{U_y^2 V_y^2} + \frac{N_1 + Z_1}{U_y^3 V_y} \Big], \quad (35)$$

where $(dy) = dy_1 dy_2 dy_3 dy_a dy_b \delta(1 - y_{123ab})$, y_1, y_2, y_3 are Feynman parameters of lepton lines, y_a, y_b are Feynman parameters of photon lines, and

$$\begin{aligned} V_y &= y_{123} + \lambda^2 y_{ab} - G, \\ G &= y_1 A_1 + y_2 A_2 + y_3 A_3, \quad \text{etc.} \end{aligned} \quad (36)$$

E_0, $\tilde{C}_0$, N_0, Z_0, N_1, Z_1 are functions of Feynman parameters defined for M_{4a} and M_{4b}, respectively. Their explicit definitions are given on pp. 266 and 267 of Ref. [29]. The *tilde* on $\tilde{C}_0$ is introduced here to avoid confusion with C_0 introduced in the definition of Π. When a VP function is inserted into the photon line a by using its spectral function representation, the denominator V_y is replaced by $V_y + y_a R(z)$. In the case of the second-order VP function P_2, where z_1, z_2 are Feynman parameters of two fermions forming the vacuum-polarization loop, we have $R(z) = m_1^2 z_{12}/(z_1 z_2)$.

For terms of Eq. (35) proportional to $1/V_y$, we can apply the substitution rule (29) directly. For the term proportional to $1/V_y^2$ we may rewrite the denominator using the formula

$$\int (dz) \frac{\rho(z)}{(V_y + y_a R(z))^2} = -\frac{\partial}{\partial V_y} \int (dz) \frac{\rho(z)}{V_y + y_a R(z)}$$

$$= \frac{\partial}{\partial V_y} \frac{\Pi(-V_y/y_a)}{V_y}$$

$$= -\frac{1}{V_y^2} \Pi(-V_y/y_a)$$

$$+ \frac{1}{V_y} \frac{\partial \Pi(-V_y/y_a)}{\partial V_y}. \tag{37}$$

This leads to the structure of the form

$$M_{4,P} = \int (dy) \left[\left(\frac{E_0 + \tilde{C}_0}{U_y^2 V_y} + \frac{N_0 + Z_0}{U_y^2 V_y^2} + \frac{N_1 + Z_1}{U_y^3 V_y} \right) \right.$$

$$\left. \times (-\Pi(-V_y/y_a)) + \frac{N_0 + Z_0}{U_y^2 V_y} \frac{\partial \Pi(-V_y/y_a)}{\partial V_y} \right]. \tag{38}$$

For $P = P_2$ we have

$$M_{4,P_2} = -\sum_{a,b} \int (dy) \int (dz) \frac{D_0}{U^2} \left[\left(\frac{E_0 + \tilde{C}_0}{U_y^2 V_y} + \frac{N_0 + Z_0}{U_y^2 V_y^2} \right. \right.$$

$$\left. \left. + \frac{N_1 + Z_1}{U_y^3 V_y} \right) \ln \left(\frac{V_0}{V} \right) + \frac{1}{y_a} \frac{N_0 + Z_0}{U_y^2 V_y} \frac{G}{V} \right], \tag{39}$$

which follows from Eq. (8) and

$$\frac{\partial \Pi^{(2)}(-V_y/y_a)}{\partial V_y} = -\frac{1}{y_a} \int (dz) \frac{D_0}{U^2} \frac{G}{V}, \tag{40}$$

where V_0 and V are given by Eq. (33), and $\sum_{a,b}$ means the sum of insertions of P_2 in photon lines a and b. Note that the structure of M_4 is largely kept intact by the insertion of Π.

For $P = P_4$, where P_4 represents P_{4a} or P_{4b}, $\Pi^{(4)}(-V_y/y_a)$ is given by Eq. (15) and its derivative can be written in the form

$$\frac{\partial \Pi^{(4)}(-V_y/y_a)}{\partial V_y} = -\frac{1}{y_a} \int (dz) \left[\frac{D_0}{U^2} \frac{G}{V^2} + \frac{C_0}{U^2} \left(\frac{1}{V} + \frac{xG}{V^2} \right) \right.$$

$$\left. + \frac{D_1}{U^3} \frac{G}{V} \right], \tag{41}$$

where, for P_{4b}, $V = V_0 - xG$, $V_0 = z_{1234}m_1^2$, $G = z_{13}A_1 + z_2A_2$, $x = -V_y/y_a$. Similarly for $P = P_{4a}$. Substituting Eqs. (15) and (41) in Eq. (38), we obtain $M_{4a(P_{4b})}$, etc. To avoid overcrowding the K operation is not shown explicitly.

A formula for $P = P_4(P_2)$, where P_4 represents P_{4a} or P_{4b}, can be readily obtained combining Eqs. (20), (22), (38), and (41):

$$M_{4,P_4(P_2)} = \int_0^1 dt \rho^{(2)}(t) \int (dy) \left[\left(\frac{E_0 + \tilde{C}_0}{U_y^2 V_y} + \frac{N_0 + Z_0}{U_y^2 V_y^2} \right. \right.$$

$$\left. + \frac{N_1 + Z_1}{U_y^3 V_y} \right)(-\Pi^{(4)}(-V_y/y_a))$$

$$\left. + \frac{N_0 + Z_0}{U_y^2 V_y} \left(\frac{\partial \Pi^{(4)}(-V_y/y_a)}{\partial V_y} \right) \right], \tag{42}$$

where V and V_0 are defined by Eq. (21).

In the case $P = P_6$, where P_6 represents one of $P_{6A}, \ldots, P_{6H}$, we obtain a formula of the form

$$M_{4,P_6} = \sum_{a,b} \int (dy) \left[\left(\frac{E_0 + \tilde{C}_0}{U_y^2 V_y} + \frac{N_0 + Z_0}{U_y^2 V_y^2} + \frac{N_1 + Z_1}{U_y^3 V_y} \right) \right.$$

$$\left. \times (-\Pi^{(6)}(-V_y/y_a)) + \frac{N_0 + Z_0}{U_y^2 V_y} \left(\frac{\partial \Pi^{(6)}(-V_y/y_a)}{\partial V_y} \right) \right], \tag{43}$$

where $\Pi^{(6)}(-V_y/y_a)$ is given by Eq. (23) and its derivative can be written in the form

$$\frac{\partial \Pi^{(6)}(-V_y/y_a)}{\partial V_y} = -\frac{1}{y_a} \int (dz) \left[\frac{2D_0}{U^2} \frac{G}{V^3} + \frac{B_0}{U^2} \left(\frac{1}{V^2} + \frac{2Gx}{V^3} \right) \right.$$

$$+ \frac{C_0}{U^2} \left(\frac{2x}{V^2} + \frac{2Gx^2}{V^3} \right) + \frac{D_1}{U^3} \frac{G}{V^2}$$

$$\left. + \frac{B_1}{U^3} \left(\frac{1}{V} + \frac{Gx}{V^2} \right) + \frac{D_2}{U^4} \frac{G}{V} \right]_{x=-V_y/y_a}. \tag{44}$$

As usual the K operation and R subtraction are assumed implicitly. The K operation removes UV-divergent parts of divergent subdiagrams from $M_{4,P_{6\alpha}}$, $\alpha = A, B, \ldots, H$, etc. Diagrams P_{6c} and P_{6d} contain a fourth-order self-energy subdiagram so that they require R subtraction in addition to K operation. The resulting finite quantities are denoted as $\Delta M_{4,P_{6\alpha}}$, etc. In order to obtain the standard result renormalized on the mass shell, further subtraction of the UV-finite remainder must be carried out by the residual renormalization.

V. SET II(C)

For the Set II(c) it is convenient to treat the renormalization of UV divergences arising from two photons forming M_{4a} and M_{4b} and the renormalization of the vacuum-polarization function separately. The first step can be written as

$$A_1^{(10)(l_1 l_2 l_3)}[\text{Set II(c)}] = \sum_{i=a,b} \Delta M_{4i,P_{4(P_2)}}^{(l_1 l_2 l_3)} - \Delta B_2 M_{2,P_{4(P_2)}}^{(l_1 l_2 l_3)}$$

$$- \Delta B_{2,P_{4(P_2)}}^{(l_1 l_2 l_3)} M_2, \tag{45}$$

where l_1, l_2, and l_3 denote the open lepton line, outer lepton loop, and inner lepton loop, respectively. The superscript l_1 is suppressed in M_2 and ΔB_2 since they are independent of

TABLE I.   Contributions of diagrams of Set II(c) to a_e for $(l_1 l_2 l_3) = (eee)$. The superscript (eee) is omitted for simplicity. The multiplicity n_F is the number of vertex diagrams represented by the integral and is incorporated in the numerical value. The top four lines are obtained by constructing the sixth-order vacuum-polarization function in terms of Feynman parameters. The bottom two lines are obtained by using the exact spectral function of the sixth order. All integrals are evaluated in double precision.

Integral	n_f	Value (Error) including n_f	Sampling per iteration	Number of iterations
$\Delta M_{4a, P_{4a(P_2)}}$	6	0.028 927 (21)	$1 \times 10^7, 1 \times 10^8$	50, 50
$\Delta M_{4a, P_{4b(P_2)}}$	12	0.004 521 (11)	$1 \times 10^7, 1 \times 10^8$	50, 50
$\Delta M_{4b, P_{4a(P_2)}}$	6	−0.110 617 (16)	$1 \times 10^7, 1 \times 10^8$	50, 50
$\Delta M_{4b, P_{4b(P_2)}}$	12	−0.020 212 (9)	$1 \times 10^7, 1 \times 10^8$	50, 50
$\Delta M_{4a, P_{4(P_2)}}$	18	0.028 425 (28)	$1 \times 10^7, 1 \times 10^8$	50, 100
$\Delta M_{4b, P_{4(P_2)}}$	18	−0.112 236 (20)	$1 \times 10^7, 1 \times 10^8$	50, 100

TABLE II.   Finite renormalization terms of Set II(c) for the case (eee). All integrals are evaluated in double precision. The quantities in the fourth line are obtained by using the exact spectral function of the sixth order. The multiplicity of the integral is incorporated in the numerical value.

Integral	Value (Error)	Integral	Value (Error)
$\Delta B_{2, P_2}$	0.063 399 266 $\cdots$	M_{2, P_2}	0.015 687 421 $\cdots$
$\Delta B_{2, P_{4a(P_2)}}$	0.047 836 (1)	$M_{2, P_{4a(P_2)}}$	0.011 403 (1)
$\Delta B_{2, P_{4b(P_2)}}$	0.008 783 (1)	$M_{2, P_{4b(P_2)}}$	0.001 717 (1)
$\Delta B_{2, P_{4(P_2)}}$	0.048 577 (5)	$M_{2, P_{4(P_2)}}$	0.011 131 (1)
$\Delta M_{4a, P_2}$	0.039 642 (42)	$\Delta M_{4b, P_2}$	−0.146 343 (35)

the lepton mass. ΔB_2 is the finite part of the second-order renormalization constant defined by $\Delta B_2 \equiv B_2^R + L_2^R$. [See Eqs. (12) and (14).] The vacuum-polarization function $P_{4(P_2)}$ is fully renormalized whose divergence structure can be readily found by the K operation. This leads to the second step:

$$\Delta M_{4i, P_{4(P_2)}}^{(l_1 l_2 l_3)} = \sum_{\beta = a,b} \Delta M_{4i, P_{4\beta(P_2)}}^{(l_1 l_2 l_3)} - 2 \Delta B_{2, P_2}^{(l_2 l_3)} \Delta M_{4i, P_2}^{(l_1 l_2)},$$

$$\text{for } i = a, b, \tag{46}$$

$$M_{2, P_{4(P_2)}}^{(l_1 l_2 l_3)} = \sum_{\beta = a,b} M_{2, P_{4\beta(P_2)}}^{(l_1 l_2 l_3)} - 2 \Delta B_{2, P_2}^{(l_2 l_3)} M_{2, P_2}^{(l_1 l_2)}, \tag{47}$$

$$\Delta B_{2, P_{4(P_2)}}^{(l_1 l_2 l_3)} = \sum_{\beta = a,b} \Delta B_{2, P_{4\beta(P_2)}}^{(l_1 l_2 l_3)} - 2 \Delta B_{2, P_2}^{(l_2 l_3)} \Delta B_{2, P_2}^{(l_1 l_2)}. \tag{48}$$

A. Numerical results: (eee) case

The contribution of Set II(c) to the electron $g - 2$ for the case $(l_1 l_2 l_3) = (eee)$, where e denotes electron, has been evaluated from Eq. (42) by three different methods:

(a) A straightforward extension of the method developed in [29],

(b) A method based on the automatic code generating algorithm GENCODEVP N [25], and

(c) Use of an exact spectral function of $\Pi^{(4,2)}$ given in Ref. [28].

All calculations are carried out by the integration routine VEGAS [34]. Preliminary evaluations of the integral (42) by the methods (a) and (b) gave results consistent with each other within the numerical uncertainty estimated by VEGAS, proving that both programs are bug-free. [Actually, both methods (a) and (b) use only K operation since R subtraction is not needed in this case.] We therefore list only the results of method (b) in the first four data lines of Table I. The values of auxiliary functions $\Delta B_{2, P_{4(P_2)}}$ and $M_{2, P_{4(P_2)}}$ are listed in Table II.

Substituting the numerical results of the integrals listed in Tables I and II in (45), we obtain

$$A_1^{(10)}[\text{Set II(c)}^{(eee)}] = -0.116 489 (32). \tag{49}$$

We also calculated the contribution of Set II(c) using the exact spectral function of $\Pi^{(4,2)}$ [28]. In this case $\Delta M_{4a, P_{4(P_2)}}^{(eee)}$, $\Delta M_{4b, P_{4(P_2)}}^{(eee)}$, $M_{2, P_{4(P_2)}}^{(eee)}$, and $\Delta B_{2, P_{4(P_2)}}^{(eee)}$ on the right-hand side of Eq. (45) can be directly evaluated using the exact spectral function. The results are listed in the last two lines of Table I and in the fourth line of Table II. The value obtained using the numbers in Tables I and II is

$$A_1^{(10)}[\text{Set II(c)}^{(eee)}: \text{spectral function}] = -0.116 447 (34), \tag{50}$$

which is in good agreement with (49). This shows that GENCODEVP N works correctly for $N = 4$.

TABLE III.   Contributions of diagrams of Set II(c) containing one electron loop and one muon loop to a_e. The superscript (eme) denotes a diagram in which the outer loop is a muon loop. The superscript (eem) denotes a diagram in which the inner loop is a muon loop. The multiplicity of the diagram n_F is included in the numerical results. All integrals are evaluated in double precision.

Integral	n_f	Value (Error) including n_f	Sampling per iteration	Number of iterations
$\Delta M^{(eme)}_{4a,P_{4a(P_2)}}$	6	0.000 017 57 (22)	1×10^7	50
$\Delta M^{(eme)}_{4a,P_{4b(P_2)}}$	12	0.000 013 37 (31)	1×10^7	50
$\Delta M^{(eme)}_{4b,P_{4a(P_2)}}$	6	$-0.000\,172\,92\,(13)$	1×10^7	50
$\Delta M^{(eme)}_{4b,P_{4b(P_2)}}$	12	$-0.000\,134\,62\,(18)$	1×10^7	50
$\Delta M^{(eem)}_{4a,P_{4a(P_2)}}$	6	0.000 014 66 (11)	1×10^7	50
$\Delta M^{(eem)}_{4a,P_{4b(P_2)}}$	12	0.000 001 73 (3)	1×10^7	50
$\Delta M^{(eem)}_{4b,P_{4a(P_2)}}$	6	$-0.000\,094\,42\,(8)$	1×10^7	50
$\Delta M^{(eem)}_{4b,P_{4b(P_2)}}$	12	$-0.000\,001\,11\,(2)$	1×10^7	50

TABLE IV.   Finite renormalization constants needed for the mass-dependent terms (e, m, e) and (e, e, m) of Set II(c). The finite renormalization constants needed for this term but not listed here can be found in Table II. All integrals are evaluated in double precision. The multiplicity of the integral is incorporated in the numerical value.

Integral	Value (Error)	Integral	Value (Error)
$\Delta B^{(eme)}_{2,P_{4a(P_2)}}$	$0.773\,326\,(53) \times 10^{-4}$	$M^{(eme)}_{2,P_{4a(P_2)}}$	$0.044\,986\,(3) \times 10^{-4}$
$\Delta B^{(eme)}_{2,P_{4b(P_2)}}$	$0.603\,167\,(106) \times 10^{-4}$	$M^{(eme)}_{2,P_{4b(P_2)}}$	$0.033\,465\,(6) \times 10^{-4}$
$\Delta B^{(eem)}_{2,P_{4a(P_2)}}$	$0.414\,245\,(42) \times 10^{-4}$	$M^{(eem)}_{2,P_{4a(P_2)}}$	$0.050\,072\,(5) \times 10^{-4}$
$\Delta B^{(eem)}_{2,P_{4b(P_2)}}$	$0.005\,000\,(9) \times 10^{-4}$	$M^{(eem)}_{2,P_{4b(P_2)}}$	$0.000\,552\,(1) \times 10^{-4}$
$\Delta M^{(em)}_{4a,P_2}$	$0.020\,90\,(21) \times 10^{-4}$	$\Delta M^{(em)}_{4b,P_2}$	$-0.209\,84\,(12) \times 10^{-4}$
$\Delta B^{(em)}_{2,P_2}$	$0.094\,050\,(3) \times 10^{-4}$	$M^{(em)}_{2,P_2}$	$0.005\,197\,62\,(21) \times 10^{-4}$
$\Delta B^{(me)}_{2,P_2}$	$1.885\,69\,(24)$		

B. Numerical results: (eme), (eee), etc.

Diagrams of Set II(c) contain two closed lepton loops, one within the other. We obtain mass-dependent contributions to the electron $g - 2$ when one or both loops consist of a muon or tau-lepton. The largest mass-dependent contributions come from the integral (45) with superscripts (eme) and then with (eem). Results of numerical integration are listed in Table III. The values obtained using the numbers in Tables III and IV are

$$A_2^{(10)}[\text{Set II(c)}^{(eme)}] = -0.260\,86\,(45) \times 10^{-3}, \qquad (51)$$

and

$$A_2^{(10)}[\text{Set II(c)}^{(eem)}] = -0.102\,63\,(14) \times 10^{-3}. \qquad (52)$$

Other mass-dependent terms of Set II(c) are listed in Table V.

C. Muon $g - 2$: (mee)

The leading contribution to the muon $g - 2$ comes from the case where both loops consist of electrons, namely, the (mee) case, where m stands for the muon. The value obtained using the numbers in Tables VI and VII is

TABLE V.   Mass-dependent contributions of diagrams of Set II(c) to the electron $g - 2$. All integrals are evaluated in double precision.

(e, l_2, l_3)	$A_2^{(10)(el_2l_3)}$	(e, l_2, l_3)	$A_3^{(10)(el_2l_3)}$
(e, m, m)	$-0.167\,65\,(28) \times 10^{-4}$	(e, m, t)	$-0.410\,01\,(81) \times 10^{-6}$
(e, t, e)	$-0.287\,97\,(58) \times 10^{-5}$	(e, t, m)	$-0.7844\,(14) \times 10^{-6}$
(e, e, t)	$-0.9889\,(20) \times 10^{-6}$		
(e, t, t)	$-0.9884\,(21) \times 10^{-7}$		

TABLE VI. Contributions to the muon $g - 2$ from Set II(c) diagrams involving closed electron and/or muon loops. The multiplicity of the diagram n_F is included in the numerical results. All integrals are evaluated in double precision.

Integral	n_f	Value (Error) including n_f	Sampling per iteration	Number of iterations
$\Delta M^{(mee)}_{4a,P_{4a(P_2)}}$	6	0.684 47 (37)	1×10^8, 1×10^9	50, 40
$\Delta M^{(mee)}_{4a,P_{4b(P_2)}}$	12	2.071 36 (55)	1×10^8, 1×10^9	50, 50
$\Delta M^{(mee)}_{4b,P_{4a(P_2)}}$	6	0.025 50 (33)	1×10^8, 1×10^9	50, 40
$\Delta M^{(mee)}_{4b,P_{4b(P_2)}}$	12	$-4.320\,77$ (51)	1×10^8, 1×10^9	50, 50
$\Delta M^{(mme)}_{4a,P_{4a(P_2)}}$	6	0.302 14 (11)	1×10^8, 1×10^9	50, 10
$\Delta M^{(mme)}_{4a,P_{4b(P_2)}}$	12	0.251 36 (19)	1×10^8, 1×10^9	50, 10
$\Delta M^{(mme)}_{4b,P_{4a(P_2)}}$	6	$-0.957\,39$ (9)	1×10^8, 1×10^9	50, 10
$\Delta M^{(mme)}_{4b,P_{4b(P_2)}}$	12	$-0.931\,56$ (15)	1×10^8, 1×10^9	50, 10
$\Delta M^{(mem)}_{4a,P_{4a(P_2)}}$	6	0.049 57 (10)	1×10^8	50
$\Delta M^{(mem)}_{4a,P_{4b(P_2)}}$	12	0.001 64 (5)	1×10^8	50
$\Delta M^{(mem)}_{4b,P_{4a(P_2)}}$	6	$-0.141\,38$ (8)	1×10^8	50
$\Delta M^{(mem)}_{4b,P_{4b(P_2)}}$	12	$-0.010\,38$ (4)	1×10^8	50

TABLE VII. Finite renormalization terms of Set II(c) for the muon anomaly a_μ. All integrals are evaluated in double precision. The multiplicity of the integral is incorporated in the numerical value.

Integral	Value (Error)	Integral	Value (Error)
$\Delta B^{(mee)}_{2,P_{4a(P_2)}}$	0.655 71 (11)	$M^{(mee)}_{2,P_{4a(P_2)}}$	0.597 441 (48)
$\Delta B^{(mee)}_{2,P_{4b(P_2)}}$	2.279 41 (17)	$M^{(mee)}_{2,P_{4b(P_2)}}$	0.982 066 (70)
$\Delta B^{(mee)}_{2,P_{4(P_2)}}$	2.695 12 (64)	$M^{(mee)}_{2,P_{4(P_2)}}$	1.440 46 (28)
$\Delta B^{(mme)}_{2,P_{4a(P_2)}}$	0.417 691 (10)	$M^{(mme)}_{2,P_{4a(P_2)}}$	0.121 908 (3)
$\Delta B^{(mme)}_{2,P_{4b(P_2)}}$	0.404 336 (22)	$M^{(mme)}_{2,P_{4b(P_2)}}$	0.099 237 (5)
$\Delta B^{(mem)}_{2,P_{4a(P_2)}}$	0.065 066 (6)	$M^{(mem)}_{2,P_{4a(P_2)}}$	0.021 016 (2)
$\Delta B^{(mem)}_{2,P_{4b(P_2)}}$	0.004 533 (3)	$M^{(mem)}_{2,P_{4b(P_2)}}$	0.000 586 (1)
$\Delta M^{(me)}_{4a,P_2}$	1.725 62 (49)	$\Delta M^{(me)}_{4b,P_2}$	$-2.354\,33$ (45)
$\Delta B^{(me)}_{2,P_2}$	1.885 732 (16)	$M^{(me)}_{2,P_2}$	1.094 258 282 7 (98)

$$A_2^{(10)}[\text{Set II(c)}^{(mee)}] = -3.888\,27\,(90). \qquad (53)$$

We checked this result using the exact spectral function:

$$A_2^{(10)}[\text{Set II(c)}^{(mee)}: \text{spectral function}] = -3.887\,65\,(92). \qquad (54)$$

D. Muon $g - 2$: (mme), (mem), and others

The next-to-leading order contribution arises when the inner and outer loops consist of an electron and muon, respectively. We found

$$A_2^{(10)}[\text{Set II(c)}^{(mme)}] = -1.345\,98\,(36). \qquad (55)$$

When the inner and outer loops consist of a muon and electron, respectively, the contribution is found to be smaller:

TABLE VIII. Contributions to the muon $g - 2$ from Set II(c) diagrams involving tau-lepton loops. All integrals are evaluated in double precision.

(m, l_2, l_3)	$A_2^{(10)(ml_2 l_3)}$	(m, l_2, l_3)	$A_3^{(10)(ml_2 l_3)}$
(m, m, t)	$-0.004\,325\,0$ (49)	(m, e, t)	$-0.004\,734\,1$ (55)
(m, t, m)	$-0.010\,519$ (13)	(m, t, e)	$-0.036\,066$ (51)
(m, t, t)	$-0.001\,504\,1$ (19)		

TABLE IX.   Contributions of diagrams of Set II(d), (*ee*) case. n_F is the number of Feynman diagrams represented by the integral. The fourth-order mass renormalization is completed by R subtraction within the numerical programs of $\Delta M_{4a,P_{6C}}$, $\Delta M_{4a,P_{6D}}$, $\Delta M_{4b,P_{6C}}$, and $\Delta M_{4b,P_{6D}}$. All integrals are evaluated in double precision.

Integral	n_f	Value (Error) including n_f	Sampling per iteration	Number of iterations
$\Delta M_{4a,P_{6A}}$	12	0.112 990 (116)	1×10^8, 1×10^9	50, 100
$\Delta M_{4a,P_{6B}}$	6	0.072 919 (72)	1×10^8, 1×10^9	50, 100
$\Delta M_{4a,P_{6C}}$	12	0.044 224 (87)	1×10^8, 1×10^9	50, 100
$\Delta M_{4a,P_{6D}}$	12	$-0.088\,822\,(78)$	1×10^8, 1×10^9	50, 100
$\Delta M_{4a,P_{6E}}$	24	0.444 033 (113)	1×10^8, 1×10^9	50, 100
$\Delta M_{4a,P_{6F}}$	12	$-0.156\,407\,(67)$	1×10^8, 1×10^9	50, 100
$\Delta M_{4a,P_{6G}}$	6	0.094 162 (54)	1×10^8, 1×10^9	50, 100
$\Delta M_{4a,P_{6H}}$	6	0.060 989 (35)	1×10^8, 1×10^9	50, 100
$\Delta M_{4b,P_{6A}}$	12	$-0.398\,926\,(66)$	1×10^8, 1×10^9	50, 100
$\Delta M_{4b,P_{6B}}$	6	$-0.253\,369\,(42)$	1×10^8, 1×10^9	50, 100
$\Delta M_{4b,P_{6C}}$	12	$-0.141\,941\,(51)$	1×10^8, 1×10^9	50, 100
$\Delta M_{4b,P_{6D}}$	12	0.292 773 (44)	1×10^8, 1×10^9	50, 100
$\Delta M_{4b,P_{6E}}$	24	$-1.395\,971\,(66)$	1×10^8, 1×10^9	50, 100
$\Delta M_{4b,P_{6F}}$	12	0.570 363 (40)	1×10^8, 1×10^9	50, 100
$\Delta M_{4b,P_{6G}}$	6	$-0.232\,467\,(32)$	1×10^8, 1×10^9	50, 100
$\Delta M_{4b,P_{6H}}$	6	$-0.223\,983\,(22)$	1×10^8, 1×10^9	50, 100

TABLE X.   Finite renormalization terms necessary for the cases (*ee*) and (*em*) of Set II(d). For simplicity the superscript (*ee*) is omitted. The values $M_{2,P_{6C}}$ and $M_{2,P_{6D}}$ are different from those in Table I of Ref. [35]. The former is constructed with the K operation and R subtraction, while the latter is with the K operation only. All integrals are evaluated in double precision.

Integral	Value (Error)	Integral	Value (Error)
$\Delta M_{4a,P_4}$	0.131 298 (8)	$\Delta M_{4b,P_4}$	$-0.420\,295\,(8)$
$\Delta M_{4a,P_2}$	0.039 642 (42)	$\Delta M_{4b,P_2}$	$-0.146\,343\,(35)$
$M_{2,P_{6A}}$	0.044 446 7 (22)	$\Delta B_{2,P_{6A}}$	0.173 609 1 (96)
$M_{2,P_{6B}}$	0.028 593 9 (14)	$\Delta B_{2,P_{6B}}$	0.110 466 1 (56)
$M_{2,P_{6C}}$	0.017 717 3 (19)	$\Delta B_{2,P_{6C}}$	0.062 134 7 (74)
$M_{2,P_{6D}}$	$-0.035\,167\,0\,(16)$	$\Delta B_{2,P_{6D}}$	$-0.127\,657\,6\,(63)$
$M_{2,P_{6E}}$	0.179 333 2 (21)	$\Delta B_{2,P_{6E}}$	0.610 385 8 (84)
$M_{2,P_{6F}}$	$-0.062\,003\,2\,(12)$	$\Delta B_{2,P_{6F}}$	$-0.247\,658\,3\,(54)$
$M_{2,P_{6G}}$	0.038 879 0 (10)	$\Delta B_{2,P_{6G}}$	0.104 070 2 (44)
$M_{2,P_{6H}}$	0.023 674 9 (8)	$\Delta B_{2,P_{6H}}$	0.097 056 7 (29)
M_{2,P_4}	$0.052\,870\,652 \cdots$	$\Delta B_{2,P_4}$	0.183 666 8 (18)
M_{2,P_2}	$0.015\,687\,421 \cdots$	$\Delta B_{2,P_2}$	$0.063\,399\,266 \cdots$
ΔLB_4	0.027 930 (27)	ΔB_2	0.75
M_2	0.5		
$\Delta M_{4a,P_4}^{(em)}$	$0.075\,96\,(78) \times 10^{-4}$	$\Delta M_{4b,P_4}^{(em)}$	$-0.757\,35\,(41) \times 10^{-4}$
$\Delta M_{4a,P_2}^{(em)}$	$0.020\,90\,(21) \times 10^{-4}$	$\Delta M_{4b,P_2}^{(em)}$	$-0.209\,84\,(12) \times 10^{-4}$
$M_{2,P_{6A}}^{(em)}$	$0.159\,949\,(32) \times 10^{-5}$	$\Delta B_{2,P_{6A}}^{(em)}$	$0.281\,371\,(61) \times 10^{-4}$
$M_{2,P_{6B}}^{(em)}$	$0.102\,323\,(21) \times 10^{-5}$	$\Delta B_{2,P_{6B}}^{(em)}$	$0.180\,003\,(40) \times 10^{-4}$
$M_{2,P_{6C}}^{(em)}$	$0.071\,033\,(29) \times 10^{-5}$	$\Delta B_{2,P_{6C}}^{(em)}$	$0.119\,848\,(52) \times 10^{-4}$
$M_{2,P_{6D}}^{(em)}$	$-0.131\,368\,(26) \times 10^{-5}$	$\Delta B_{2,P_{6D}}^{(em)}$	$-0.226\,651\,(46) \times 10^{-4}$
$M_{2,P_{6E}}^{(em)}$	$0.682\,404\,(32) \times 10^{-5}$	$\Delta B_{2,P_{6E}}^{(em)}$	$1.162\,709\,(59) \times 10^{-4}$
$M_{2,P_{6F}}^{(em)}$	$-0.211\,985\,(19) \times 10^{-5}$	$\Delta B_{2,P_{6F}}^{(em)}$	$-0.379\,345\,(35) \times 10^{-4}$
$M_{2,P_{6G}}^{(em)}$	$0.174\,650\,(16) \times 10^{-5}$	$\Delta B_{2,P_{6G}}^{(em)}$	$0.279\,935\,(31) \times 10^{-4}$
$M_{2,P_{6H}}^{(em)}$	$0.082\,748\,(12) \times 10^{-5}$	$\Delta B_{2,P_{6H}}^{(em)}$	$0.147\,672\,(22) \times 10^{-4}$
$M_{2,P_4}^{(em)}$	$0.197\,298\,(5) \times 10^{-5}$	$\Delta B_{2,P_4}^{(em)}$	$0.338\,738\,(12) \times 10^{-4}$
$M_{2,P_2}^{(em)}$	$0.051\,974\,(1) \times 10^{-5}$	$\Delta B_{2,P_2}^{(em)}$	$0.094\,050\,(3) \times 10^{-4}$

TABLE XI.   Contributions to a_e from diagrams of Set II(d) containing a muon loop. The superscript (*em*) signifies that the diagrams contain a muon loop in the electron $g - 2$. n_F is the number of Feynman diagrams represented by the integral. All integrals are evaluated in double precision. The fourth-order mass renormalization is completed within the numerical programs of $\Delta M_{4a,P_{6C}}$, $\Delta M_{4a,P_{6D}}$, $\Delta M_{4b,P_{6C}}$, and $\Delta M_{4b,P_{6D}}$.

Integral	n_f	Value (Error) including n_f	Sampling per iteration	Number of iterations
$\Delta M_{4a,P_{6A}}^{(em)}$	12	0.000 006 24 (13)	1×10^7, 1×10^8	50, 50
$\Delta M_{4a,P_{6B}}^{(em)}$	6	0.000 004 94 (9)	1×10^7, 1×10^8	50, 50
$\Delta M_{4a,P_{6C}}^{(em)}$	12	0.000 003 79 (11)	1×10^7, 1×10^8	50, 50
$\Delta M_{4a,P_{6D}}^{(em)}$	12	0.000 005 23 (10)	1×10^7, 1×10^8	50, 50
$\Delta M_{4a,P_{6E}}^{(em)}$	24	0.000 026 34 (15)	1×10^7, 1×10^8	50, 50
$\Delta M_{4a,P_{6F}}^{(em)}$	12	0.000 008 38 (8)	1×10^7, 1×10^8	50, 50
$\Delta M_{4a,P_{6G}}^{(em)}$	6	0.000 007 54 (6)	1×10^7, 1×10^8	50, 50
$\Delta M_{4a,P_{6H}}^{(em)}$	6	0.000 003 34 (5)	1×10^7, 1×10^8	50, 50
$\Delta M_{4b,P_{6A}}^{(em)}$	12	0.000 063 78 (4)	1×10^7, 1×10^8	50, 50
$\Delta M_{4b,P_{6B}}^{(em)}$	6	0.000 040 16 (2)	1×10^7, 1×10^8	50, 50
$\Delta M_{4b,P_{6C}}^{(em)}$	12	0.000 027 79 (3)	1×10^7, 1×10^8	50, 50
$\Delta M_{4b,P_{6D}}^{(em)}$	12	0.000 051 62 (3)	1×10^7, 1×10^8	50, 50
$\Delta M_{4b,P_{6E}}^{(em)}$	24	0.000 260 81 (4)	1×10^7, 1×10^8	50, 50
$\Delta M_{4b,P_{6F}}^{(em)}$	12	0.000 085 61 (2)	1×10^7, 1×10^8	50, 50
$\Delta M_{4b,P_{6G}}^{(em)}$	6	0.000 063 72 (2)	1×10^7, 1×10^8	50, 50
$\Delta M_{4b,P_{6H}}^{(em)}$	6	0.000 033 95 (1)	1×10^7, 1×10^8	50, 50

$$A_2^{(10)}[\text{Set II(c)}^{(mem)}] = -0.151\,50\,(15). \qquad (56)$$

The contributions involving tau-lepton loops are summarized in Table VIII.

VI. SET II(D)

Following the same consideration leading to Eq. (45) of Sec. V we obtain

$$A_1^{(10)}[\text{Set II(d)}^{(l_1 l_2)}] = \sum_{i=a}^{b} \Delta M_{4i,P_6}^{(l_1 l_2)} - \Delta B_2 M_{2,P_6}^{(l_1 l_2)}$$
$$- \Delta B_{2,P_6}^{(l_1 l_2)} M_2, \qquad (57)$$

where l_2 designates the loop lepton. The vacuum-polarization function P_6 is fully renormalized whose divergence structure can be readily found by the K operation. The renormalization formula for P_6 takes different forms depending on whether one follows the original K operation prescription[29] or the K operation plus R subtraction method [19]. In the first approach the UV-finite part of the fourth-order mass-renormalization term is not subtracted when P_{6C} and P_{6D} are constructed. In the second approach we subtract the mass-renormalization

term completely, including the finite part $\Delta \delta m_4$, which leads to

$$\Delta M_{4i,P_6}^{(l_1 l_2)} = \sum_{\beta=A}^{H} \Delta M_{4i,P_{6\beta}}^{(l_1 l_2)} - 4\Delta B_2 \Delta M_{4i,P_4}^{(l_1 l_2)}$$
$$- 3(\Delta B_2)^2 \Delta M_{4i,P_2}^{(l_1 l_2)} - 2\Delta LB_4 \Delta M_{4i,P_2}^{(l_1 l_2)},$$
$$\text{for } i = a, b,$$

$$M_{2,P_6}^{(l_1 l_2)} = \sum_{\beta=A}^{H} M_{2,P_{6\beta}}^{(l_1 l_2)} - 4\Delta B_2 M_{2,P_4}^{(l_1 l_2)} - 3(\Delta B_2)^2 M_{2,P_2}^{(l_1 l_2)}$$
$$- 2\Delta LB_4 M_{2,P_2}^{(l_1 l_2)},$$

$$\Delta B_{2,P_6}^{(l_1 l_2)} = \sum_{\beta=A}^{H} \Delta B_{2,P_{6\beta}}^{(l_1 l_2)} - 4\Delta B_2 \Delta B_{2,P_4}^{(l_1 l_2)} - 3(\Delta B_2)^2 \Delta B_{2,P_2}^{(l_1 l_2)}$$
$$- 2\Delta LB_4 \Delta B_{2,P_2}^{(l_1 l_2)}. \qquad (58)$$

The quantities on the right-hand-side of (58), $\Delta M_{4i,P_{6\beta}}$, $\Delta B_{2,P_{6\beta}}$, and $M_{2,P_{6\beta}}$, are defined by the K operation and R subtraction. ΔLB_4 is the sum of the finite parts of the fourth-order vertex-renormalization constant ΔL_4 and wave-function renormalization constant ΔB_4. See Refs. [3,4,29] for the exact definition. Note that terms

like $\Delta M_{4i,P_{6\beta}}$ include the multiplicity n_F of Feynman diagrams that contribute to them.

A. Numerical results: (*ee*) case

Preliminary calculations of the (*ee*) case based on methods (a) and (b) described in Sec. VA are consistent with each other within the uncertainty estimated by VEGAS. Therefore we list only the results of method (b) in Table IX. From this table and Table X we obtain

$$A_1^{(10)}[\text{Set II(d)}^{(ee)}] = -0.243\,00\,(29). \qquad (59)$$

The Padé-approximated vacuum-polarization function of the sixth order with a single fermion loop has been obtained in Refs. [30,31]. This method gives both imaginary and real parts of the vacuum-polarization function. We use here only its imaginary part to calculate its effect on the anomaly. Numerical results of integration are summarized in Table XII. Substituting them into Eq. (57), we obtained

$$A_1^{(10)}[\text{Set II(d)}^{(ee)}: \text{Padé}] = -0.243\,06\,(45), \qquad (60)$$

which is in good agreement with (59). This provides another support for the validity of GENCODEVP N.

B. Numerical results: Mass-dependent terms (*em*) and (*et*)

The value of the mass-dependent term (*em*) obtained using the numbers listed in Table XI is

$$A_2^{(10)}[\text{Set II(d)}^{(em)}] = -0.9817\,(42) \times 10^{-4}. \qquad (61)$$

As a check we evaluated the same quantity using the Padé-approximated vacuum-polarization function of sixth-order. The results are listed in Table XII. From these values we obtain

TABLE XII. Contributions of diagrams of Set II(d) whose VP function is P_6. Quantities on the right-hand-side of Eq. (58) are calculated from Tables IX, X, XI, XIII, XIV, and XV. The same quantities are also calculated by the Padé approximant method and listed with the subscript Padé below the corresponding integrals. $M_{2,P6}^{(l_1 l_2)}$ are actually the anomaly contributions of the eighth-order diagrams of Group I(d). Their values for the (*ee*) and (*me*) cases are consistent with Eq. (29) of Ref. [35] and Eq. (34) of Ref. [5], respectively. The (*em*), (*et*), and (*mt*) cases are newly evaluated in this paper. All integrals using the Padé approximant are evaluated in quadruple precision.

Integral	Value (Error)	Integral	Value (Error)
$\Delta M_{4a,P_6}^{(ee)}$	0.119 08 (25)	$\Delta M_{4b,P_6}^{(ee)}$	$-0.264\,51\,(41)$
$\Delta M_{4a,P_6\text{Padé}}^{(ee)}$	0.118 95 (35)	$\Delta M_{4b,P_6\text{Padé}}^{(ee)}$	$-0.264\,43\,(27)$
$\Delta B_{2,P_6}^{(ee)}$	0.120 879 (20)	$M_{2,P_6}^{(ee)}$	0.049 514 (5)
$\Delta B_{2,P_6\text{Padé}}^{(ee)}$	0.120 862 (39)	$M_{2,P_6\text{Padé}}^{(ee)}$	0.049 520 (4)
$\Delta M_{4a,P_6}^{(em)}$	$0.0915\,(39) \times 10^{-4}$	$\Delta M_{4b,P_6}^{(em)}$	$-0.8620\,(16) \times 10^{-4}$
$\Delta M_{4a,P_6\text{Padé}}^{(em)}$	$0.091\,96\,(53) \times 10^{-4}$	$\Delta M_{4b,P_6\text{Padé}}^{(em)}$	$-0.872\,25\,(31) \times 10^{-4}$
$\Delta B_{2,P_6}^{(em)}$	$0.385\,36\,(13) \times 10^{-4}$	$M_{2,P_6}^{(em)}$	$0.024\,725\,(7) \times 10^{-4}$
$\Delta B_{2,P_6\text{Padé}}^{(em)}$	$0.385\,367\,(72) \times 10^{-4}$	$M_{2,P_6\text{Padé}}^{(em)}$	$0.024\,727\,(4) \times 10^{-4}$
$\Delta M_{4a,P_6\text{Padé}}^{(et)}$	$0.039\,89\,(154) \times 10^{-6}$	$\Delta M_{4b,P_6\text{Padé}}^{(et)}$	$-0.470\,90\,(74) \times 10^{-6}$
$\Delta B_{2,P_6\text{Padé}}^{(et)}$	$0.210\,278\,(39) \times 10^{-6}$	$M_{2,P_6\text{Padé}}^{(et)}$	$0.008\,744\,(1) \times 10^{-6}$
$\Delta M_{4a,P_6}^{(me)}$	$-0.4694\,(50)$	$\Delta M_{4b,P_6}^{(me)}$	0.5969 (42)
$\Delta M_{4a,P_6\text{Padé}}^{(me)}$	$-0.4591\,(55)$	$\Delta M_{4b,P_6\text{Padé}}^{(me)}$	0.5935 (51)
$\Delta B_{2,P_6}^{(me)}$	$-0.394\,72\,(82)$	$M_{2,P_6}^{(me)}$	$-0.229\,82\,(36)$
$\Delta B_{2,P_6\text{Padé}}^{(me)}$	$-0.395\,25\,(78)$	$M_{2,P_6\text{Padé}}^{(me)}$	$-0.230\,23\,(32)$
$\Delta M_{4a,P_6}^{(mt)}$	0.001 066 (15)	$\Delta M_{4b,P_6}^{(mt)}$	$-0.006\,953\,(10)$
$\Delta M_{4a,P_6\text{Padé}}^{(mt)}$	0.001 065 (12)	$\Delta M_{4b,P_6\text{Padé}}^{(mt)}$	$-0.006\,953\,(8)$
$\Delta B_{2,P_6}^{(mt)}$	0.003 020 9 (10)	$M_{2,P_6}^{(mt)}$	0.000 367 7 (2)
$\Delta B_{2,P_6\text{Padé}}^{(mt)}$	0.003 021 4 (6)	$M_{2,P_6\text{Padé}}^{(mt)}$	0.000 367 7 (1)

TABLE XIII.   Leading contributions of diagrams of Set II(d) of Fig. 1 to the muon $g - 2$. n_F is the number of Feynman diagrams represented by the integral. All integrals are evaluated in double precision. The fourth-order mass renormalization is completed within the numerical programs of $\Delta M_{4a,P_{6C}}$, $\Delta M_{4a,P_{6D}}$, $\Delta M_{4b,P_{6C}}$, and $\Delta M_{4b,P_{6D}}$. The last two columns list initial sampling and its iteration, followed by increased sampling and its iteration.

Integral	n_f	Value (Error) including n_f	Sampling per iteration	Number of iterations
$\Delta M_{4a,P_{6A}}^{(me)}$	12	10.6935 (20)	1×10^8, 1×10^9, 1×10^{10}	50, 100, 135
$\Delta M_{4a,P_{6B}}^{(me)}$	6	5.6421 (12)	1×10^8, 1×10^9, 1×10^{10}	50, 100, 120
$\Delta M_{4a,P_{6C}}^{(me)}$	12	4.3050 (12)	1×10^8, 1×10^9, 1×10^{10}	50, 100, 120
$\Delta M_{4a,P_{6D}}^{(me)}$	12	$-6.0977\,(12)$	1×10^8, 1×10^9, 1×10^{10}	50, 100, 120
$\Delta M_{4a,P_{6E}}^{(me)}$	24	$-4.3659\,(18)$	1×10^8, 1×10^9, 1×10^{10}	50, 100, 120
$\Delta M_{4a,P_{6F}}^{(me)}$	12	$-6.145\,99\,(94)$	1×10^8, 1×10^9, 1×10^{10}	50, 100, 120
$\Delta M_{4a,P_{6G}}^{(me)}$	6	$-0.3977\,(14)$	1×10^8, 1×10^9, 1×10^{10}	50, 100, 120
$\Delta M_{4a,P_{6H}}^{(me)}$	6	5.048 76 (52)	1×10^8, 1×10^9, 1×10^{10}	50, 100, 50
$\Delta M_{4b,P_{6A}}^{(me)}$	12	$-18.9591\,(16)$	1×10^8, 1×10^9, 1×10^{10}	50, 100, 120
$\Delta M_{4b,P_{6B}}^{(me)}$	6	$-9.815\,33\,(96)$	1×10^8, 1×10^9, 1×10^{10}	50, 100, 100
$\Delta M_{4b,P_{6C}}^{(me)}$	12	$-7.998\,86\,(93)$	1×10^8, 1×10^9, 1×10^{10}	50, 100, 100
$\Delta M_{4b,P_{6D}}^{(me)}$	12	11.248 41 (81)	1×10^8, 1×10^9, 1×10^{10}	50, 100, 100
$\Delta M_{4b,P_{6E}}^{(me)}$	24	15.9050 (12)	1×10^8, 1×10^9, 1×10^{10}	50, 100, 120
$\Delta M_{4b,P_{6F}}^{(me)}$	12	7.177 72 (74)	1×10^8, 1×10^9, 1×10^{10}	50, 100, 100
$\Delta M_{4b,P_{6G}}^{(me)}$	6	$-0.501\,22\,(94)$	1×10^8, 1×10^9, 1×10^{10}	50, 100, 110
$\Delta M_{4b,P_{6H}}^{(me)}$	6	$-8.025\,32\,(40)$	1×10^8, 1×10^9, 1×10^{10}	50, 100, 50

TABLE XIV.   Contribution from diagrams of Set II(d) (m, t) of Fig. 1 to the muon $g - 2$. n_F is the number of Feynman diagrams represented by the integral. All integrals are evaluated in double precision. The last two columns list initial sampling and its iteration, followed by increased sampling and its iteration.

Integral	n_f	Value (Error) including n_f	Sampling per iteration	Number of iterations
$\Delta M_{4a,P_{6A}}^{(mt)}$	12	0.001 746 1 (22)	1×10^8, 1×10^9	50, 100
$\Delta M_{4a,P_{6B}}^{(mt)}$	6	0.000 476 4 (14)	1×10^8, 1×10^9	50, 100
$\Delta M_{4a,P_{6C}}^{(mt)}$	12	0.000 323 9 (18)	1×10^8, 1×10^9	50, 100
$\Delta M_{4a,P_{6D}}^{(mt)}$	12	$-0.001\,605\,3\,(17)$	1×10^8, 1×10^9	50, 100
$\Delta M_{4a,P_{6E}}^{(mt)}$	24	0.003 112 4 (24)	1×10^8, 1×10^9	50, 100
$\Delta M_{4a,P_{6F}}^{(mt)}$	12	$-0.002\,000\,0\,(13)$	1×10^8, 1×10^9	50, 100
$\Delta M_{4a,P_{6G}}^{(mt)}$	6	0.001 766 5 (12)	1×10^8, 1×10^9	50, 100
$\Delta M_{4a,P_{6H}}^{(mt)}$	6	0.000 390 55 (72)	1×10^8, 1×10^9	50, 100
$\Delta M_{4b,P_{6A}}^{(mt)}$	12	$-0.006\,549\,50\,(87)$	1×10^8, 1×10^9	50, 100
$\Delta M_{4b,P_{6B}}^{(mt)}$	6	$-0.004\,550\,21\,(57)$	1×10^8, 1×10^9	50, 100
$\Delta M_{4b,P_{6C}}^{(mt)}$	12	$-0.002\,299\,84\,(74)$	1×10^8, 1×10^9	50, 100
$\Delta M_{4b,P_{6D}}^{(mt)}$	12	0.004 413 20 (67)	1×10^8, 1×10^9	50, 100
$\Delta M_{4b,P_{6E}}^{(mt)}$	24	$-0.022\,437\,50\,(93)$	1×10^8, 1×10^9	50, 100
$\Delta M_{4b,P_{6F}}^{(mt)}$	12	0.008 566 26 (53)	1×10^8, 1×10^9	50, 100
$\Delta M_{4b,P_{6G}}^{(mt)}$	6	$-0.005\,164\,07\,(46)$	1×10^8, 1×10^9	50, 100
$\Delta M_{4b,P_{6H}}^{(mt)}$	6	$-0.003\,940\,06\,(31)$	1×10^8, 1×10^9	50, 100

TABLE XV. Finite renormalization terms needed for Set II(d) of the muon $g - 2$. Both (me) and (mt) cases are listed. $M_{2,P_{6\beta}}^{(me)}$ with $\beta = A, B, E, F, G, H$ are consistent with those in Ref. [5]. $M_{2,P_{6\beta}}$ with $\beta = C, D$ in this table incorporated the R subtraction [19] and differ from those in Ref. [5].

Integral	Value (Error)	Integral	Value (Error)
$\Delta M_{4a,P_4}^{(me)}$	2.047 84 (23)	$\Delta M_{4b,P_4}^{(me)}$	−2.486 60 (12)
$\Delta M_{4a,P_2}^{(me)}$	1.725 62 (49)	$\Delta M_{4b,P_2}^{(me)}$	−2.354 33 (46)
$M_{2,P_{6A}}^{(me)}$	5.676 49 (22)	$\Delta B_{2,P_{6A}}^{(me)}$	11.500 82 (47)
$M_{2,P_{6B}}^{(me)}$	3.058 13 (13)	$\Delta B_{2,P_{6B}}^{(me)}$	6.101 83 (27)
$M_{2,P_{6C}}^{(me)}$	2.194 66 (12)	$\Delta B_{2,P_{6C}}^{(me)}$	4.616 02 (24)
$M_{2,P_{6D}}^{(me)}$	−3.224 25 (10)	$\Delta B_{2,P_{6D}}^{(me)}$	−6.701 64 (22)
$M_{2,P_{6E}}^{(me)}$	−0.073 76 (17)	$\Delta B_{2,P_{6E}}^{(me)}$	−4.076 72 (36)
$M_{2,P_{6F}}^{(me)}$	−4.064 09 (9)	$\Delta B_{2,P_{6F}}^{(me)}$	−6.535 49 (20)
$M_{2,P_{6G}}^{(me)}$	−0.246 97 (12)	$\Delta B_{2,P_{6G}}^{(me)}$	−0.039 85 (28)
$M_{2,P_{6H}}^{(me)}$	2.838 67 (4)	$\Delta B_{2,P_{6H}}^{(me)}$	5.345 15 (8)
$M_{2,P_4}^{(me)}$	1.493 671 581 (8)	$\Delta B_{2,P_4}^{(me)}$	2.439 109 (53)
$M_{2,P_2}^{(me)}$	1.094 258 282 7 (98)	$\Delta B_{2,P_2}^{(me)}$	1.885 733 (16)
$\Delta M_{4a,P_4}^{(mt)}$	0.000 903 9 (47)	$\Delta M_{4b,P_4}^{(mt)}$	−0.006 571 6 (31)
$\Delta M_{4a,P_2}^{(mt)}$	0.000 247 8 (15)	$\Delta M_{4b,P_2}^{(mt)}$	−0.001 888 8 (10)
$M_{2,P_{6A}}^{(mt)}$	0.000 239 71 (1)	$\Delta B_{2,P_{6A}}^{(mt)}$	0.002 436 62 (13)
$M_{2,P_{6B}}^{(mt)}$	0.000 153 39 (1)	$\Delta B_{2,P_{6B}}^{(mt)}$	0.001 558 94 (8)
$M_{2,P_{6C}}^{(mt)}$	0.000 106 19 (1)	$\Delta B_{2,P_{6C}}^{(mt)}$	0.001 006 23 (11)
$M_{2,P_{6D}}^{(mt)}$	−0.000 196 75 (1)	$\Delta B_{2,P_{6D}}^{(mt)}$	−0.001 934 79 (9)
$M_{2,P_{6E}}^{(mt)}$	0.001 021 35 (1)	$\Delta B_{2,P_{6E}}^{(mt)}$	0.009 826 56 (12)
$M_{2,P_{6F}}^{(mt)}$	−0.000 318 06 (1)	$\Delta B_{2,P_{6F}}^{(mt)}$	−0.003 326 19 (7)
$M_{2,P_{6G}}^{(mt)}$	0.000 260 44 (1)	$\Delta B_{2,P_{6G}}^{(mt)}$	0.002 250 09 (6)
$M_{2,P_{6H}}^{(mt)}$	0.000 124 05 (1)	$\Delta B_{2,P_{6H}}^{(mt)}$	0.001 292 36 (4)
$M_{2,P_4}^{(mt)}$	0.000 295 508 (21)	$\Delta B_{2,P_4}^{(mt)}$	0.002 880 01 (31)
$M_{2,P_2}^{(mt)}$	0.000 078 067 4 (31)	$\Delta B_{2,P_2}^{(mt)}$	0.000 831 107 (75)

$$A_2^{(10)}[\text{Set II(d)}^{(em)}: \text{Padé}] = -0.99153\,(61) \times 10^{-4}. \quad (62)$$

We also evaluated the mass-dependent term (et) in Padé approximation:

$$A_2^{(10)}[\text{Set II(d)}^{(et)}: \text{Padé}] = -0.5427\,(18) \times 10^{-6}. \quad (63)$$

We have not evaluated this term directly. But it will be of the same order as Eq. (63) and thus negligible numerically.

C. Muon $g - 2$: (me)

The leading contribution to the muon $g - 2$ comes from the case (me). The value obtained using the numbers in Tables X, XIII, and XV is

$$A_2^{(10)}[\text{Set II(d)}^{(me)}] = 0.4972\,(65). \quad (64)$$

This is in fair agreement with the value obtained using the Padé approximant

$$A_2^{(10)}[\text{Set II(d)}^{(me)}: \text{Padé}] = 0.5048\,(75). \quad (65)$$

A crude evaluation of the contribution of the tau-lepton loop gives

$$A_2^{(10)}[\text{Set II(d)}^{(mt)}] = -0.007\,673\,(18), \quad (66)$$

while the same contribution obtained using the Padé approximant is

$$A_2^{(10)}[\text{Set II(d)}^{(mt)}: \text{Padé}] = -0.007\,674\,(15). \quad (67)$$

VII. SUMMARY AND DISCUSSION

The total contribution to a_e from the Set II(c) is the sum of Eqs. (49), (51), and (52), and other terms listed in Table V:

$$a_e^{(10)}[\text{Set II(c): all}] = -0.116\,874\,(43)\left(\frac{\alpha}{\pi}\right)^5. \quad (68)$$

Contributions of the tau-lepton loop listed in Table VIII are less than the uncertainty of Eq. (68).

The total contribution to a_e from the Set II(d) is the sum of Eqs. (59) and (61):

$$a_e^{(10)}[\text{Set II(d): all}] = -0.243\,10\,(29)\left(\frac{\alpha}{\pi}\right)^5. \quad (69)$$

The contribution of the tau-lepton loop is within the error bars of Eq. (69) and is completely negligible at present.

The total contribution of Set II(c) to the muon $g - 2$ involving electron, muon, and tau-lepton loops is the sum of Eq. (49), Eqs. (53), (55), and (56), and values listed in Table V:

$$a_\mu^{(10)}[\text{Set II(c): all}] = -5.5594\,(11)\left(\frac{\alpha}{\pi}\right)^5. \quad (70)$$

The total contribution of Set II(d) to the muon $g - 2$ involving electron, muon, and tau-lepton loops is the sum of Eqs. (59), (64), and (66):

$$a_\mu^{(10)}[\text{Set II(d): all}] = 0.2465\,(65)\left(\frac{\alpha}{\pi}\right)^5. \quad (71)$$

The sum of the electron-loop contribution to the muon $g - 2$ from the diagrams Set II(c) and Set II(d) is the sum of Eqs. (53), (55), (56), and (64). We find

$$A_2^{(10)}(m_\mu/m_e)[\text{Set II(c + d)}^{(me)}] = -4.8886\,(65), \quad (72)$$

which is less than 1% of the leading contribution from the diagrams of Set VI(a) that contain light-by-light-scattering subdiagrams and vacuum-polarization subdiagrams [5,36]. Hence, the new contribution does not alter the previous estimates:

$$A_2^{(10)}(m_\mu/m_e)[\text{estimate: Ref.[5]}] = 663\,(20), \quad (73)$$

$$A_2^{(10)}(m_\mu/m_e)[\text{estimate: Ref.[36]}] = 643\,(20). \quad (74)$$

ACKNOWLEDGMENTS

[1] D. Hanneke, S. Fogwell, and G. Gabrielse, Phys. Rev. Lett. **100**, 120801 (2008).

[2] D. Hanneke, S. Fogwell Hoogerheide, and G. Gabrielse, arXiv:1009.4831.

[3] T. Aoyama, M. Hayakawa, T. Kinoshita, and M. Nio, Phys. Rev. Lett. **99**, 110406 (2007).

[4] T. Aoyama, M. Hayakawa, T. Kinoshita, and M. Nio, Phys. Rev. D **77**, 053012 (2008).

[5] T. Kinoshita and M. Nio, Phys. Rev. D **73**, 053007 (2006).

[6] B. Krause, Phys. Lett. B **390**, 392 (1997).

[7] K. Melnikov and A. Vainshtein, Phys. Rev. D **70**, 113006 (2004).

[8] M. Davier, A. Höcker, B. Malaescu, and Z. Zhang, Eur. Phys. J. C **71**, 1515 (2011).

[9] T. Teubner, K. Hagiwara, R. Liao, A. D. Martin, and D. Nomura, in Proceedings of the PhiPsi09 Conference, 2009, Beijing, China.

[10] J. Bijnens and J. Prades, Mod. Phys. Lett. A **22**, 767 (2007).

[11] J. Prades, E. de Rafael, and A. Vainshtein, arXiv:0901.0306.

[12] A. Nyffeler, Phys. Rev. D **79**, 073012 (2009).

[13] M. Knecht, S. Peris, M. Perrottet, and E. De Rafael, J. High Energy Phys. 11 (2002) 003.

[14] A. Czarnecki, W. J. Marciano, and A. Vainshtein, Phys. Rev. D **67**, 073006 (2003); **73**, 119901(E) (2006).

[15] A. Czarnecki, B. Krause, and W. J. Marciano, Phys. Rev. Lett. **76**, 3267 (1996).

[16] R. Bouchendira, P. Clade, S. Guellati-Khelifa, F. Nez, and F. Biraben, Phys. Rev. Lett. **106** 080801 (2011).

[17] P. J. Mohr, B. N. Taylor, and D. B. Newell, Rev. Mod. Phys. **80**, 633 (2008).

[18] T. Aoyama, M. Hayakawa, T. Kinoshita, and M. Nio, Nucl. Phys. **B740**, 138 (2006).

[19] T. Aoyama, M. Hayakawa, T. Kinoshita, and M. Nio, Nucl. Phys. **B796**, 184 (2008).

[20] T. Kinoshita and M. Nio, Phys. Rev. D **70**, 113001 (2004).

[21] T. Aoyama, M. Hayakawa, T. Kinoshita, M. Nio, and N. Watanabe, Phys. Rev. D **78**, 053005 (2008).

[22] T. Aoyama, M. Hayakawa, T. Kinoshita, and M. Nio, Phys. Rev. D **78**, 113006 (2008).

[23] T. Aoyama, K. Asano, M. Hayakawa, T. Kinoshita, M. Nio, and N. Watanabe, Phys. Rev. D **81**, 053009 (2010).

[24] T. Aoyama, M. Hayakawa, T. Kinoshita, and M. Nio, Phys. Rev. D **82**, 113004 (2010).

[25] T. Aoyama, M. Hayakawa, T. Kinoshita, and M. Nio, Phys. Rev. D **83**, 053003 (2011).

[26] S. Laporta, Phys. Lett. B **328**, 522 (1994).

[27] J.-P. Aguilar, E. de Rafael, and D. Greynat, Phys. Rev. D **77**, 093010 (2008).

[28] A. H. Hoang, J. H. Kuhn, and T. Teubner, Nucl. Phys. **B452**, 173 (1995).

[29] T. Kinoshita, in *Quantum Electrodynamics*, edited by T. Kinoshita, Advanced Series on Directions in High Energy Physics Vol. 7 (World Scientific, Singapore, 1990), p. 218.

[30] P. A. Baikov and D. J. Broadhurst, arXiv:hep-ph/9504398.

[31] T. Kinoshita and M. Nio, Phys. Rev. D **60**, 053008 (1999).

[32] T. Kinoshita and M. Nio, Phys. Rev. Lett. **82**, 3240 (1999); **103**, 079901(E) (2009).

[33] T. Kinoshita and W. B. Lindquist, Phys. Rev. D **27**, 853 (1983).

[34] G. P. Lepage, J. Comput. Phys. **27**, 192 (1978).

[35] T. Kinoshita and M. Nio, Phys. Rev. D **73**, 013003 (2006).

[36] A. Kataev, Phys. Rev. D **74**, 073011 (2006).